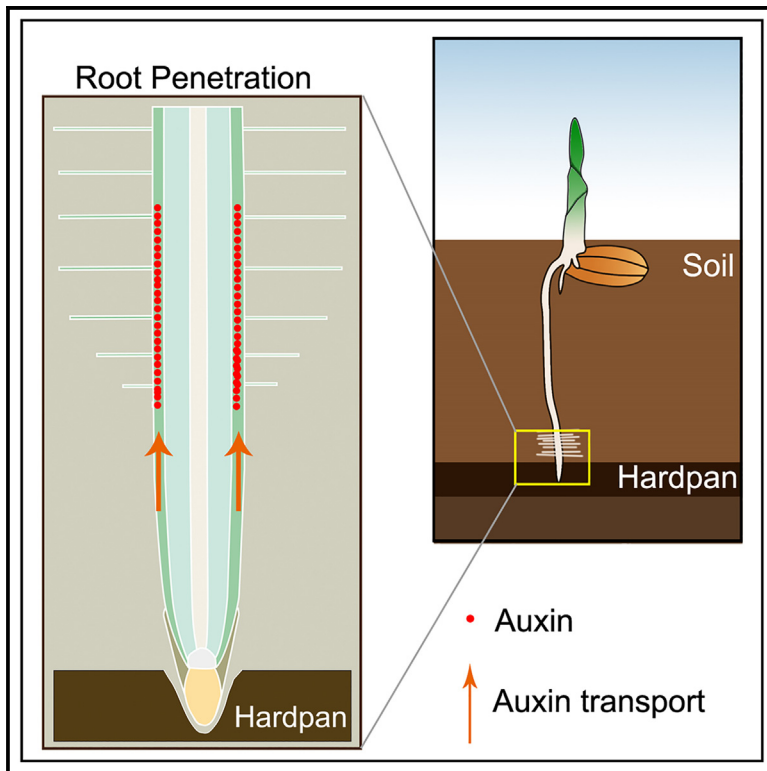


Current Biology

Root hairs facilitate rice root penetration into compacted layers

Graphical abstract



Authors

Xiuzhen Kong, Suhang Yu,
Yali Xiong, ..., Malcolm J. Bennett,
Bipin K. Pandey, Guoqiang Huang

Correspondence

bipin.pandey@nottingham.ac.uk (B.K.P.),
huang19880901@sjtu.edu.cn (G.H.)

In brief

Kong et al. provide evidence for the anchorage functions of root hairs in root penetration, a process that is regulated by OsYUC8-mediated auxin biosynthesis and OsAUX1-mediated auxin transport when roots encounter a compacted barrier.

Highlights

- Mechanical impedance induced the upregulation of auxin biosynthesis in root apex
- Auxin transport from root tip to hair zone promoted root penetration via root hair
- Mutants of *OsYUC8* and *OsAUX1* had trouble penetrating into the compacted layer
- Increased root hair length provided greater anchorage force for root penetration



Article

Root hairs facilitate rice root penetration into compacted layers

Xiuzhen Kong,^{1,4,5} Suhang Yu,^{1,5} Yali Xiong,¹ Xiaoyun Song,¹ Lucia Nevescanin-Moreno,² Xiaoqing Wei,³ Jinliang Rao,¹ Hu Zhou,³ Malcolm J. Bennett,² Bipin K. Pandey,^{2,*} and Guoqiang Huang^{1,6,*}

¹Joint International Research Laboratory of Metabolic & Developmental Sciences, State Key Laboratory of Hybrid Rice, SJTU-University of Adelaide Joint Centre for Agriculture and Health, School of Life Sciences and Biotechnology, Shanghai Jiao Tong University, 200240 Shanghai, China

²Plant and Crop Science Division, School of Biosciences, University of Nottingham, Nottingham LE12 5RD, UK

³Key Laboratory of Arable Land Conservation (North China), Ministry of Agriculture, College of Land Science and Technology, China Agricultural University, Beijing, China

⁴Shanghai Collaborative Innovation Center of Agri-Seeds/School of Agriculture and Biology, Shanghai Jiao Tong University, 200240 Shanghai, China

⁵These authors contributed equally

⁶Lead contact

*Correspondence: bipin.pandey@nottingham.ac.uk (B.K.P.), huang19880901@sjtu.edu.cn (G.H.)

<https://doi.org/10.1016/j.cub.2024.03.064>

SUMMARY

Compacted soil layers adversely affect rooting depth and access to deeper nutrient and water resources, thereby impacting climate resilience of crop production and global food security. Root hair plays well-known roles in facilitating water and nutrient acquisition. Here, we report that root hair also contributes to root penetration into compacted layers. We demonstrate that longer root hair, induced by elevated auxin response during a root compaction response, improves the ability of rice roots to penetrate harder layers. This compaction-induced auxin response in the root hair zone is dependent on the root apex-expressed auxin synthesis gene *OsYUCCA8* (*OsYUC8*), which is induced by compaction stress. This auxin source for root hair elongation relies on the auxin influx carrier *AUXIN RESISTANT 1* (*OsAUX1*), mobilizing this signal from the root apex to the root hair zone. Mutants disrupting *OsYUC8* and *OsAUX1* genes exhibit shorter root hairs and weaker penetration ability into harder layers compared with wild type (WT). Root-hair-specific mutants phenocopy these auxin-signaling mutants, as they also exhibit an attenuated root penetration ability. We conclude that compaction stress upregulates *OsYUC8*-mediated auxin biosynthesis in the root apex, which is subsequently mobilized to the root hair zone by *OsAUX1*, where auxin promotes root hair elongation, improving anchorage of root tips to their surrounding soil environment and aiding their penetration ability into harder layers.

INTRODUCTION

A large proportion of arable land exhibits vulnerability to soil compaction stress, which represents a major challenge to agriculture and food security.^{1,2} Compacted subsoil layers adversely affect root downward growth,³ thereby impeding access to water and mobile nutrients at greater depths. The mechanical impedance of compacted layers constitutes a significant challenge, imposing physical and physiological limitations on plant growth, including diminished stomatal aperture, leaf size, plant height, and yield.^{4,5} The reduction in biomass observed in crops grown in compacted soil is attributable in part to the impact of impaired root penetration and resource capture.^{6,7} In order to tackle these challenges, it is imperative to cultivate crops that possess an augmented capacity to penetrate compacted soils.¹ This is of particular significance given the projected global population of 10 billion by 2050.⁸ Thus, developing crops that can better penetrate compacted soils promises to aid food security efforts in the coming decades.

Identifying root adaptive mechanisms that aid penetration of compacted soil is vital.⁹ When roots come across a compacted soil layer, they are confronted with two potential outcomes: either penetrate the layer or deviate from their initial growth trajectory.¹⁰ In situations where the root lacks adequate lateral support or anchorage strength, the root tips bend above the compacted layer, impeding their access to deeper resources.¹¹ This provision of anchorage strength is purportedly facilitated by root hair, which are elongated, tubular outgrowths originating from root epidermal cells.^{12,13} Root hair has long been attributed to enhancing the interactions between roots and soil, leading to increased water absorption and nutrient uptake.¹⁴ Despite the common association of root hair with anchorage during seedling establishment,^{9,13} their functional roles during root penetration of compacted soil remain less explored.

In this study, we explore how root hair serves as a crucial component aiding rice root penetration of compacted layers. We report, when encountering compacted layers, how root tip expression of the auxin synthesis gene *OsYUC8* is upregulated,



increasing auxin levels that are mobilized by the auxin transporter OsAUX1 to the root hair zone. The attenuation of auxin responses in the root hair zone of mutants lacking *OsYUC8* and *OsAUX1* reduces their ability to penetrate compacted layers. Moreover, two root hair mutants also diminished root penetration capacity akin to mutants of *OsYUC8* and *OsAUX1*. Collectively, the augmentation of auxin response in roots induced by compaction stress stimulated root hair elongation, aiding anchorage required for enhanced root penetration ability in compacted layers.

RESULTS

Rice root growth trajectory is altered when encountering a compacted layer

Compacted soils typically feature elevated mechanical strength due to increased bulk density (BD), resulting in decreased gas diffusion.^{15,16} This reduction impedes ethylene diffusion out from root tissues, triggering root growth inhibition.¹⁵ The impact of high soil strength on root growth also imposes water stress (matric potential),^{17,18} rendering it challenging to discern whether the plant is responding to low water availability, high soil strength, or both.^{7,15} To address this concern, we have devised an agar-based synthetic screening system to specifically study barrier strength, which has been extensively employed in the examination of mechanical strength in *Arabidopsis*.^{11,19,20} This comprises a standardized system using agar composed of a top layer of 1% agar and a bottom layer of 3% agar. By integrating a high-density agar gel layer to simulate the hardpan (high-strength layer) present in compacted soils (Figure 1A), we have generated a partial barrier that emulates the mechanical impedance encountered by roots.

To evaluate the capacity of root penetration through a strong layer, we monitored root growth angle and length after mechanical impedance. Following a growth period of 5 days, we observed that the growth of wild-type (WT) (cv. Nipponbare [Nip]) rice roots was impeded at higher levels of compaction (3% agar, as depicted in Figure 1B), consistent with previous studies conducted in soil.^{21,22} We here chose 3% agar to study mechanical impedance responses, as 3% agar was sufficient to reduce the root growth up to 25% as compared with 1% agar. Notably, in our split system (1%/3% agar, as illustrated in Figure 1B), roots exhibit curvature after encountering the boundary, indicating that an increase in mechanical impedance (stress) alters root growth angle.

Auxin acts downstream of ethylene in modulating root elongation through compacted soil²³ and also controlling root angle.²⁴ To investigate whether auxin plays a role in the root's response to mechanical stress, we utilized the DR5-VENUS reporter to reveal changes in auxin response during this adaptive growth process.²⁴ Confocal imaging revealed an elevated auxin response in the root apex and epidermal cells in the elongation zone of WT (cv. Dong Jin [DJ]) roots upon encountering the barrier (Figures 1C–1E). Our observations suggest mechanical impedance triggers a local auxin response in root tip tissues, but it is unclear how this elevated auxin response is mediated.

OsYUC8-mediated auxin biosynthesis regulates root penetration through barriers

YUC family members control auxin biosynthesis via the conversion of indole-3-pyruvic acid (IPA) to indole-3-acetic acid (IAA) in

plants.²⁵ Among the 14 members in rice, *OsYUC8* was found to play a major role in regulating primary root growth.²⁶ Consistently, only *OsYUC8* was induced by mechanical impedance compared with other root-expressed *OsYUC* genes, including *OsYUC3*, *OsYUC5*, and *OsYUC11* (Figure 2A). In order to localize the expression of *OsYUC8*, a *GUS* reporter gene was transcriptionally fused to a 3.0 kb fragment upstream of the *OsYUC8* start codon. Histochemical analysis revealed that the localized *GUS* signals were predominately accumulated at the root apex of transgenic plants (Figure 2B). This *OsYUC8* reporter revealed a significant elevation in *GUS* activity when roots encountered a stronger layer (Figures 2C and 2D), suggesting that its expression was induced in response to mechanical impedance. Given this pattern of expression of *OsYUC8* in root apex, it is plausible that the induction of higher auxin response by root tissues encountering mechanical impedance depends on *OsYUC8*-mediated auxin biosynthesis.

To experimentally verify the *OsYUC8*-mediated model, we crossed the rice DR5-VENUS auxin reporter into the *osyuc8-2* background, a T-DNA insertion knockout mutant.²⁶ The fluorescence intensity of the DR5-VENUS reporter in epidermal cells of differentiated zone of WT (cv. Hwayoung [HWY]) was observed to be reduced in *osyuc8-2* roots, particularly after encountering the harder agar layer (Figures 3A and 3B). Consistently, mechanical impedance-induced expression of *OslAA20*, an auxin-responsive gene,²⁴ yet it remains unchanged in *osyuc8-2* (Figure 3C). Hence, the upregulation of auxin response observed in root tip tissues following mechanical impedance is dependent on *OsYUC8*.

To test the physiological function of *OsYUC8*-mediated auxin biosynthesis in root response to strong layers, we tested whether *osyuc8-2* roots exhibited an altered response after encountering a stronger agar barrier. This revealed that *osyuc8-2* plants grown in a split system exhibited significantly greater bending angles than their WT background (Figures 3D–3G). To test if other *OsYUC* family members are required to mediate auxin biosynthesis during the root response to mechanical impedance, we employed a specific auxin biosynthesis inhibitor called yucasin, which specially inhibits the function of YUC proteins.²⁷ Significantly, roots of both WT and *osyuc8-2* mutants treated with yucasin displayed a comparable phenotype to untreated *osyuc8-2* controls (Figures 3D–3G). Hence, *OsYUC8*-mediated auxin biosynthesis is specifically required to facilitate root penetration into harder layers.

Next, we investigated whether the root penetration deficiency of *osyuc8-2* lines could be ascribed to a compromised gravitropic response. However, *osyuc8-2* and WT roots exhibited comparable gravitropic responses, regardless of yucasin treatment (Figures 4A–4C). Hence, another root characteristic regulated by *OsYUC8* appears to promote rice root ability to penetrate harder layers. Root hair elongation is known to be regulated by auxin²⁸ and is linked with improved soil penetration during seedling establishment.¹³ Examination of root hair length revealed that they are much longer in WT roots grown in the split (1%/3%) system compared with lower-compaction (1%/1%) system (Figures 4D–4L). However, induction of root hair length by the split system was completely suppressed in the roots of *osyuc8-2*, and *osyuc8-2* and WT treated with yucasin (Figures 4D–4L). These findings suggest *OsYUC8*-mediated

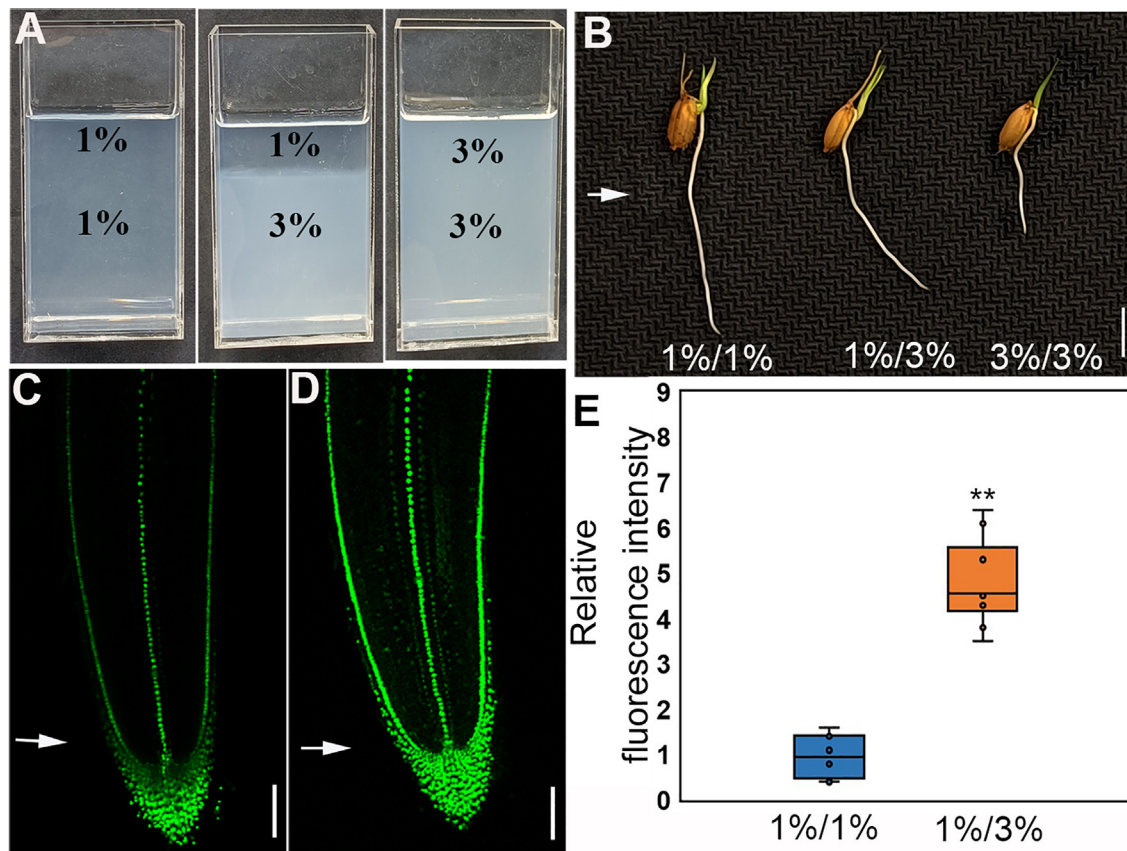


Figure 1. Increasing growth media hardness changes root growth direction and enhances auxin responses

(A) Representative images of the system (uniform systems: [1%/1% and 3%/3% agar systems] and split system: [upper system: 1% agar; lower system: 3% agar]) used in this work.

(B) Representative images of WT (cv. Nip) grown in uniform (1%/1% and 3%/3% agar) and split (1%/3% agar) systems. Scale bar represents 1 cm. White arrow indicates the split barrier position.

(C and D) Representative confocal images at median plane of primary root tips of rice auxin sensor (DR5-VENUS) cultured in 1%/1% (C) and 1%/3% (D) agar systems. Scale bars represent 100 μm . White arrows indicate the split barrier positions.

(E) Boxplot exhibiting the relative fluorescence intensity of VENUS signals in the root tip of WT grown in 1%/1% and 1%/3% agar systems. $n = 11$. Student's t test: $**p < 0.01$.

See also Figures S1 and S2.

auxin promotion of root hair elongation may aid rice root penetration when encountering harder layers.

The *OsAUX1* mutation disrupts rice root penetration into harder layers

Auxin-mediated promotion of rice root hair elongation is dependent on *OsAUX1* to facilitate auxin transport from the root apex to the root hair zone.²⁸ To examine the impact of the *osaux1* mutation on the induction of the auxin response when encountering a harder layer, we compared DR5-VENUS expression in WT versus mutant backgrounds. In contrast to WT, *osaux1-3* displayed no change in the DR5-VENUS auxin response reporter when mutant root tips encountered the boundary of the harder layer (Figures 5A–5E). These findings reveal that the elevated auxin responses triggered by the mechanical impedance were disrupted in the root epidermal cells of the *osaux1-3* mutant. Consequently, *osaux1-3* provides a useful genetic tool to explore the functional importance of the elevated auxin response in the root elongation zone during penetration of harder layers.

As anticipated, WT treated with yucasin and *osaux1-3* mutant roots exhibit quicker elongation compared with WT under uniform impedance conditions (i.e., 1%:1% or 3%:3%; Figures 5F–5J), which is consistent with previous findings in compacted soil.²³ However, *osaux1-3* mutant roots exhibited a reduced ability to penetrate harder agar layers (1%/3%) and instead featured a horizontal growth pattern along the boundary of the high-strength agar layer (Figures 5F–5I and 5K). This behavior was in contrast to the successful penetration by WT (cv. DJ) roots into the high-strength agar layers (Figures 5F–5I and 5K). Moreover, *osaux1-3* exhibits less response to external yucasin treatment (Figures 5F–5K). Mutational studies indicate that the increased auxin responses in the elongation zone, which is reliant on *OsAUX1*-mediated shootward auxin transport, also play a crucial role in facilitating root penetration into harder layers.

How can *OsAUX1* facilitate root penetration into harder layers? *OsAUX1*-mediated shootward auxin transport is required for root gravitropism and root hair elongation in response to environmental stimuli.²⁸ Consistently, *osaux1-3* exhibits a reduced

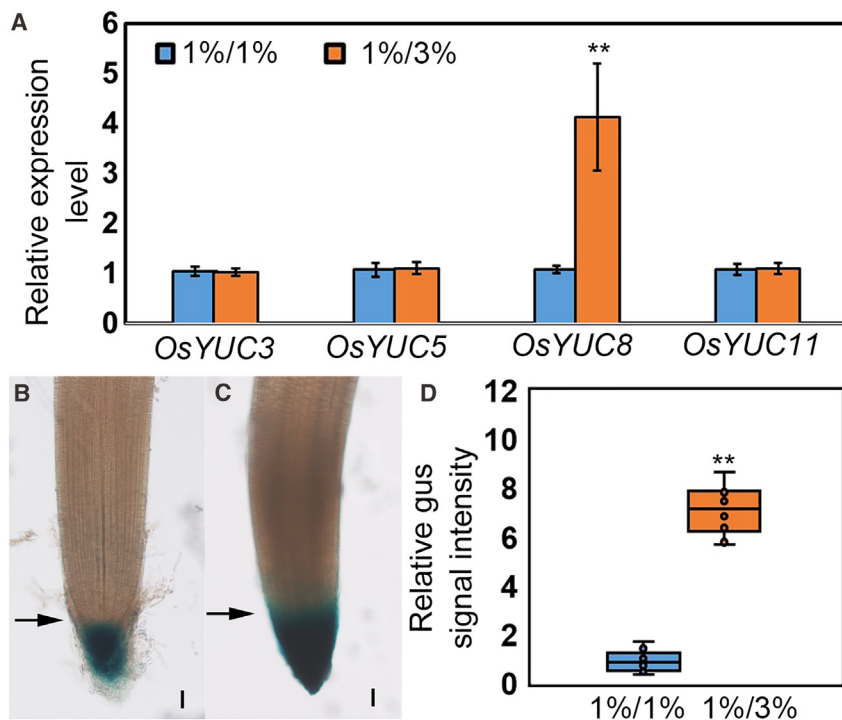


Figure 2. *ProOsYUC8::GUS* exhibits higher expression when encountering mechanical impedance

(A) Relative expression level of *OsYUCs* in the root tip of WT grown in 1%/1% and 1%/3% agar systems. Error bars are \pm SE, $n = 3$. Student's *t* test: ** $p < 0.01$.

(B and C) Representative images of rice *proOsYUC8::GUS* transcriptional reporter grown in 1%/1% (B) and 1%/3% (C) agar systems. Scale bars, 1 cm. Black arrows indicate the split barrier positions.

(D) Quantitative analysis of relative GUS signal intensity for *proOsYUC8::GUS* lines cultured in 1%/1% and 1%/3% agar systems. $n = 10$. Student's *t* test: ** $p < 0.01$.

gravitropic response, as evidenced by a bending angle of approximately 30° , in contrast to the approximately 90° exhibited by the WT (Figures S1A and S1B). The *osaux1-3* mutant also displays shorter root hairs (but with a normal number of root hair) in the split system compared with the WT (Figures S1C–S1H), indicating that the elongation of root hair in response to encountering a harder layer is dependent on *OsAUX1*. Although it is plausible that the defective penetration ability of *osaux1-3* into harder layers was attributable to the mutant's reduced gravitropic response, it appears more likely that the impaired length of *osaux1* root hair disrupts root penetration into compacted layers (through decreased anchorage).

Our results imply auxin plays a crucial role modulating root penetration by promoting root hair elongation. To further verify this, we examined the effects of auxin treatment on the root penetration ability of auxin mutants, *osyuc8* and *osaux1*, when challenged with our compacted layer bioassay. We observed that the defective penetration phenotypes observed in these mutants were effectively restored after exogenous treatment with the synthetic auxin 1-Naphthaleneacetic acid (1-NAA; Figures S2A–S2F). Furthermore, the penetration ability of WT (cv. DJ) was further increased following auxin treatment (Figures S2D–S2F). Consistently, longer root hairs were observed in WT, and defects in root hair length of auxin mutants were completely restored upon auxin treatment (Figures S2G–S2P). Taken together, it appears plausible that auxin promotes root penetration by promoting root hair elongation.

Root hair mutants exhibit reduced root penetration ability

To determine whether root hair elongation (rather than gravitropism) was important for enabling roots to penetrate harder layers, we next characterized rice mutants that specifically disrupt

root hair elongation. Mutant lines were characterized for *root hairless1* (*RHL1*), which encodes a novel basic-helix-loop-helix (bHLH) transcription factor expressed exclusively in root hair cells.²⁹ The root hair length of *rhl1-1* is significantly reduced in comparison with WT (cv. Kasalath [Kas]).²⁹ Similarly, *cellulose synthase-like D1* (*CSLD1*) gene is expressed solely in root hair cells.³⁰ Compared with WT (cv. DJ), Root hairs of *csld1* are shorter, but there is no defect in root hair density.³⁰ To

validate their root-hair-specific expression patterns, promoter fragments of *RHL1* and *CSLD1* were fused to the VENUS-N7 nuclei reporter, confirming that they were exclusively detected in root hair cell nuclei (Figures S3A–S3D). Consequently, *rhl1-1* and *csld1* mutants, which exhibit root-hair-specific defects, were deployed to evaluate the contribution of root hair in helping roots penetrate harder layers.

When grown in a uniform-hardness split agar system, the root length of *rhl1-1* and *csld1* mutants was comparable to their respective WT backgrounds (Figure S3E), indicating root elongation ability of root hair mutants is unimpaired under these constant impedance conditions. Furthermore, root hair mutants and WT plants showed no discernible differences in their root gravitropic responses (Figures S3F–S3J), further supporting their specific role in root hair development. To assess the impact of root hair on the ability of roots to penetrate stronger layers, we grew root hair mutants in the split system. We observed only a minor deviation in growth trajectory of WT roots; by contrast, root hair mutants exhibited enhanced bending (Figures 6A and 6B). Furthermore, it is observed that root hair mutants do not display any response to external auxin treatment (Figure S4), suggesting that root hair genes function downstream of auxin in the regulation of root-hair-mediated root penetration. This finding suggests that root hair mutants encountered difficulties penetrating harder layers, which is reminiscent of the phenotype observed in *osyuc8-2* (Figures 3D–3G).

Root hairs are reported to aid seedling establishment through providing anchorage for emerging roots to penetrate the soil surface.¹³ Quantification of the maximum reaction force (anchorage) provided by root hairs is frequently based on the force required to extract a root. In uniform systems, the force needed to pull out a WT root was significantly greater than that required for root hair mutants across different densities of agar

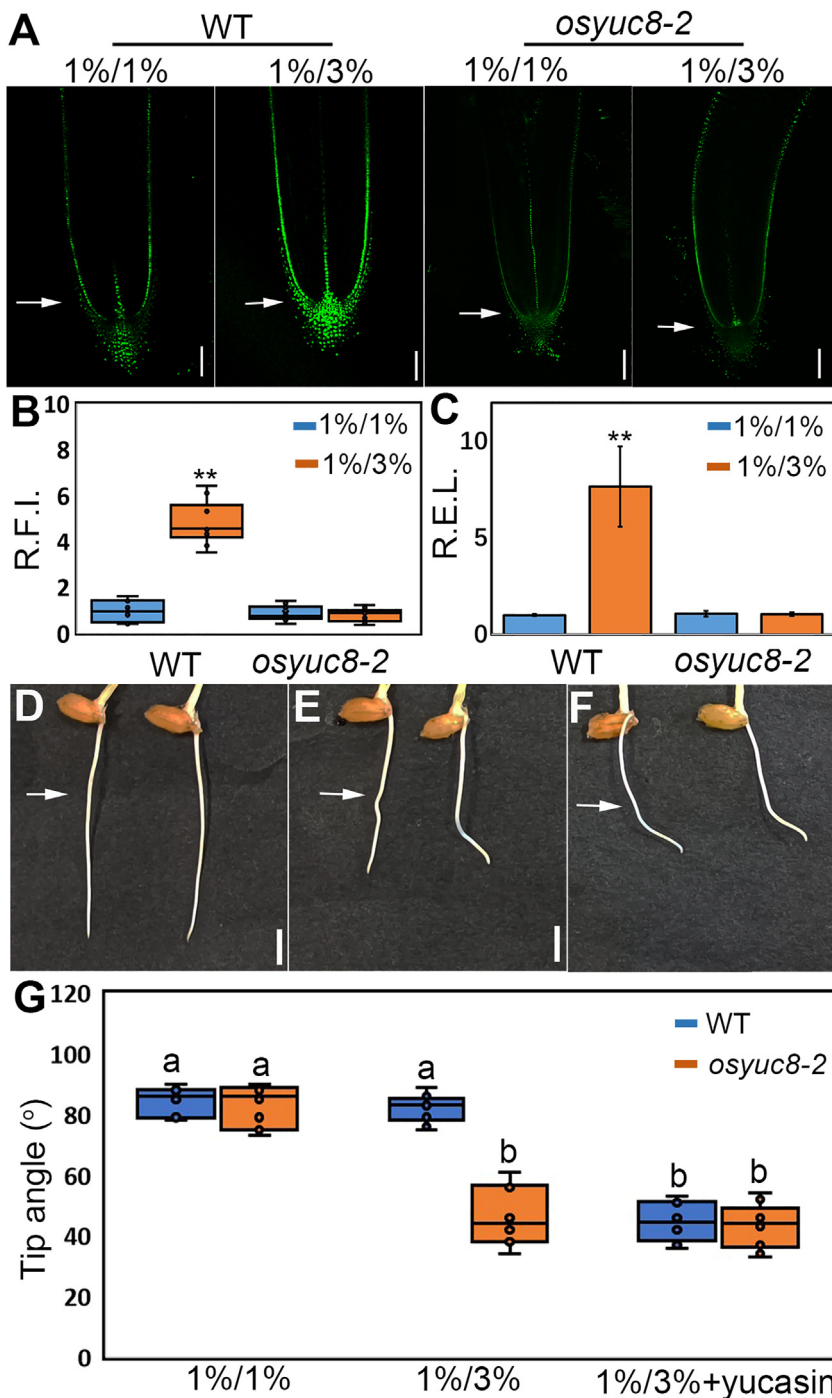


Figure 3. The *osyuc8-2* mutant exhibits reduced root penetration ability

(A) Representative confocal images captured at median plane of WT (cv. HWY) and *osyuc8-2* primary root tips of rice auxin biosensor (DR5-VENUS) grown in 1%/1% and 1%/3% agar systems. Scale bars represent 100 μ m. White arrows indicate the split barrier positions.

(B) Boxplot exhibiting the relative fluorescence intensity (R.F.I.) of VENUS signals in the root tip of WT and *osyuc8-2* grown in 1%/1% and 1%/3% systems. $n = 10$. Student's *t* test: ** $p < 0.01$.

(C) Relative expression level (R.E.L.) of *OsAA20* in the root tip of WT and *osyuc8-2* grown in 1%/1% and 1%/3% systems. Error bars are \pm SE, $n = 3$. Student's *t* test: ** $p < 0.01$.

(D–F) Representative images of WT (left) and *osyuc8-2* (right) primary root tips grown in uniform (1%/1%, D) and split (1%/3%, E and 1%/3% with 20 μ M yucasin, F) systems. Scale bars represent 1 cm. White arrows indicate the split barrier positions.

(G) Boxplot showing the root growth angle of WT and *osyuc8-2* grown in 1%/1% and 1%/3% with/without 20 μ M yucasin systems. $n = 10$. Different letters indicate significant difference, $p < 0.01$ from one-way analysis of variance (ANOVA) with Tukey's multiple comparison test.

See also [Figure S2](#).

WT lines when encountering a compacted soil layer (Figures 6C–6G; Videos S2, S3, S4, and S5). This altered root growth behavior resembled what was observed in the artificial agar-based system (Figure 6A). Additionally, root hairs were shorter in mutants compared with WT (Figures 6H–6L). Our findings reveal that root hair elongation is necessary for effective root penetration into compacted layers. We conclude that compacted layers induce elevated auxin biosynthesis and transport to the root hair zone. This, in turn, leads to the formation of longer root hairs, which provide enhanced anchorage for root penetration.

DISCUSSION

Compacted soil, particularly in the form of a hardpan, is prevalent in lowland rice fields and hinders the penetration of roots to deeper soil layers.^{31,32} As a result, nutrient uptake is reduced,

and rain-fed crops become more susceptible to drought stress.³² In this work, we demonstrate impedance-induced promotion of root hair length plays a crucial role in anchoring growing roots and aiding their penetration of compacted layers. In addition, we report the molecular mechanisms underlying the elongation response of root hair to compacted layers facilitated by auxin (Figure 6M). The presence of strong agar layers triggers the induction of *OsYUC8*, a key gene involved in auxin biosynthesis, leading to an elevated auxin concentration at the root apex. Subsequently,

layers (Figure S5). Our findings support that increased root hair lengths enhance the anchorage of growing root tips to penetrate harder layers.

To investigate whether rice root hair mutants exhibit comparable penetration defects in both split agar- and soil-based systems, we imaged root hair mutants growing through compacted layers of varying bulk densities (upper: 1.0 g cm^{-3} BD; lower 1.4 g cm^{-3} BD; Figure S6; Video S1). Using micro-computed tomography (CT), we observed that root hair mutants displayed a sharp “S-shape” in their root growth direction compared with

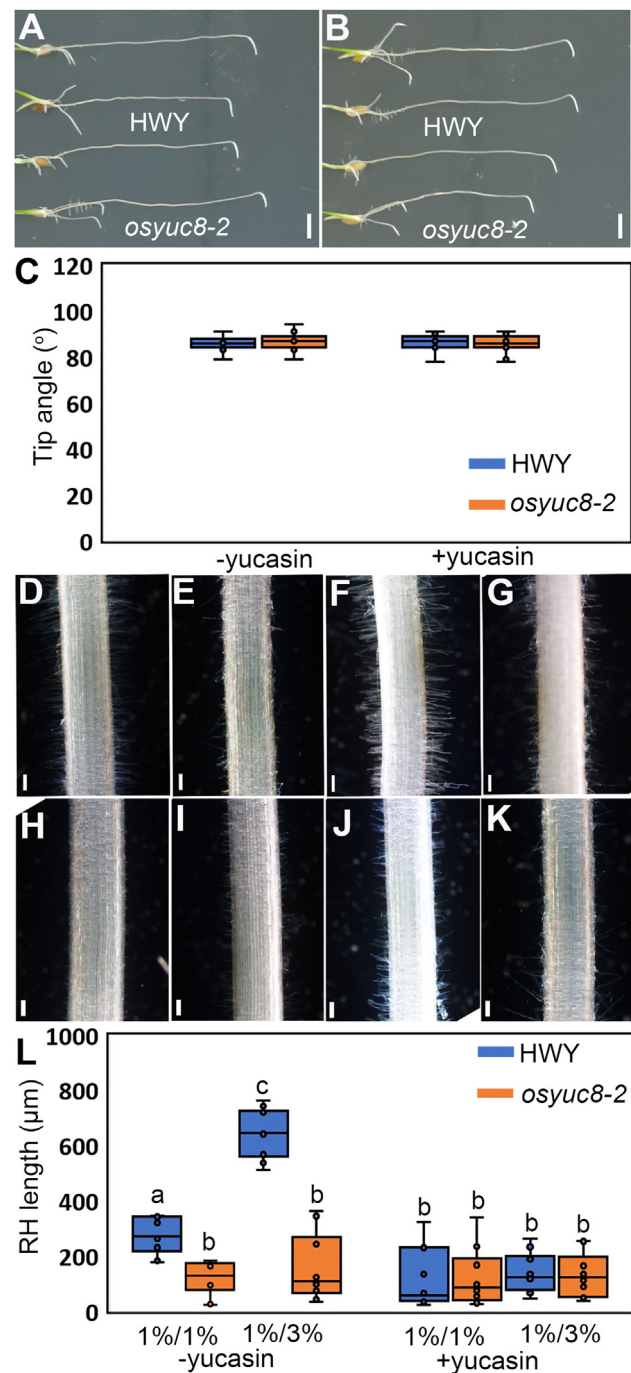


Figure 4. The *osyuc8-2* mutant exhibits reduced root hair length

(A and B) Representative images of WT (cv. HWY) and *osyuc8-2* primary roots without (A) or with (B) 20 μ M yucasin treatment when exposed to 8-h gravity stimulation. Scale bars, 1 cm.

(C) Tip angle analysis of WT and *osyuc8-2* with/without 20 μ M yucasin treatment after 8-h gravitropism. $n = 10$.

(D and E) Representative images of WT (D) and *osyuc8-2* (E) root hair (RH) at 1%/1% system without 20 μ M yucasin treatment. Scale bars represent 500 μ m.

(F and G) Representative images of WT (F) and *osyuc8-2* (G) RH at 1%/3% systems without 20 μ M yucasin treatment. Scale bars represent 500 μ m.

(H and I) Representative images of WT (H) and *osyuc8-2* (I) RH at 1%/1% system with 20 μ M yucasin treatment. Scale bars represent 500 μ m.

this auxin is transported via OsAUX1 from the root apex to the differentiation zone, promoting the elongation of root hair. The elongation of root hair results in an increased surface area of root-soil contact, generating the required anchorage force to support root penetration into compacted layers. Our previous research has also unveiled the pivotal role of OsAUX1 in facilitating root hair elongation under low phosphate conditions.²⁸ This process is crucial for transporting auxin back to the differentiation zone, where root hair elongation takes place. This finding underscores the possibility that longer root hair in compacted soil may have contributed to enhanced phosphate uptake.³³ These results collectively indicate that AUX1-mediated root hair elongation is a conserved mechanism across different plant species and under a diverse array of environmental conditions.

Previous studies have demonstrated that reduced ethylene diffusion in compacted soil leads to the accumulation of auxin and abscisic acid (ABA) in root tip tissues, thereby inhibiting root elongation within compacted soils.^{15,23} Mutants of the related hormone-signaling genes exhibit better elongation ability within compacted soil.^{15,23} In line with these findings, our research also indicates that mutants of auxin transport genes do not exhibit a response to uniform compaction conditions (Figures 5F–5J). However, mutants with disrupted auxin biosynthesis and transport pathways display reduced penetration ability into compacted layers, accompanied by significant changes in growth trajectory (Figures 3D–3G, 5F–5I, and 5K). These observations suggest that successful root penetration is reliant on rice roots' ability to avoid bending when encountering a hard layer. Hence, differences in the ability of rice roots to penetrate compacted layers are not solely determined by their elongation ability in strong soil but also by their capacity to overcome mechanical impedance when faced with a rapid increase in soil resistance.

Our study reports that increased root auxin responses in strong agar layers are dependent on the induction of OsYUC8-mediated auxin biosynthesis at the root apex and subsequent OsAUX1-mediated shootward auxin transport, triggering auxin-responsive markers like *OsIAA20* (Figure 3C). Disrupting OsYUC8 blocked upregulation of auxin-responsive markers, revealing the importance of auxin biosynthesis (rather than auxin catabolism and response). The mechanistic basis of OsYUC8 upregulation after encountering mechanical impedance remains unclear (Figure 2). Mechanical stimulation induces higher expression of the mechano-inducible calcium channel PIEZO1 (PZO1) in columella and lateral root cap cells in *Arabidopsis*.²⁰ Furthermore, *pzo1* seedlings exhibited reduced calcium transients and failed to penetrate hard agar, indicating the involvement of PZO1 in the root's short-term response to mechanical detection of compacted soil layers.^{20,34} This calcium-signaling pathway may act upstream of auxin (and OsYUC8) in the root barrier-touching response.

(J and K) Representative images of WT (J) and *osyuc8-2* (K) RH at 1%/3% system with 20 μ M yucasin treatment. Scale bars represent 500 μ m.

(L) Boxplot showing RH length analysis of WT and *osyuc8-2* grown in uniform and split agar systems with/without 20 μ M yucasin treatment. $n = 10$ representative RHs from 10 individual roots. Different letters indicate significant differences, $p < 0.01$ from one-way analysis of variance (ANOVA) with Tukey's multiple comparison test.

See also Figure S2.

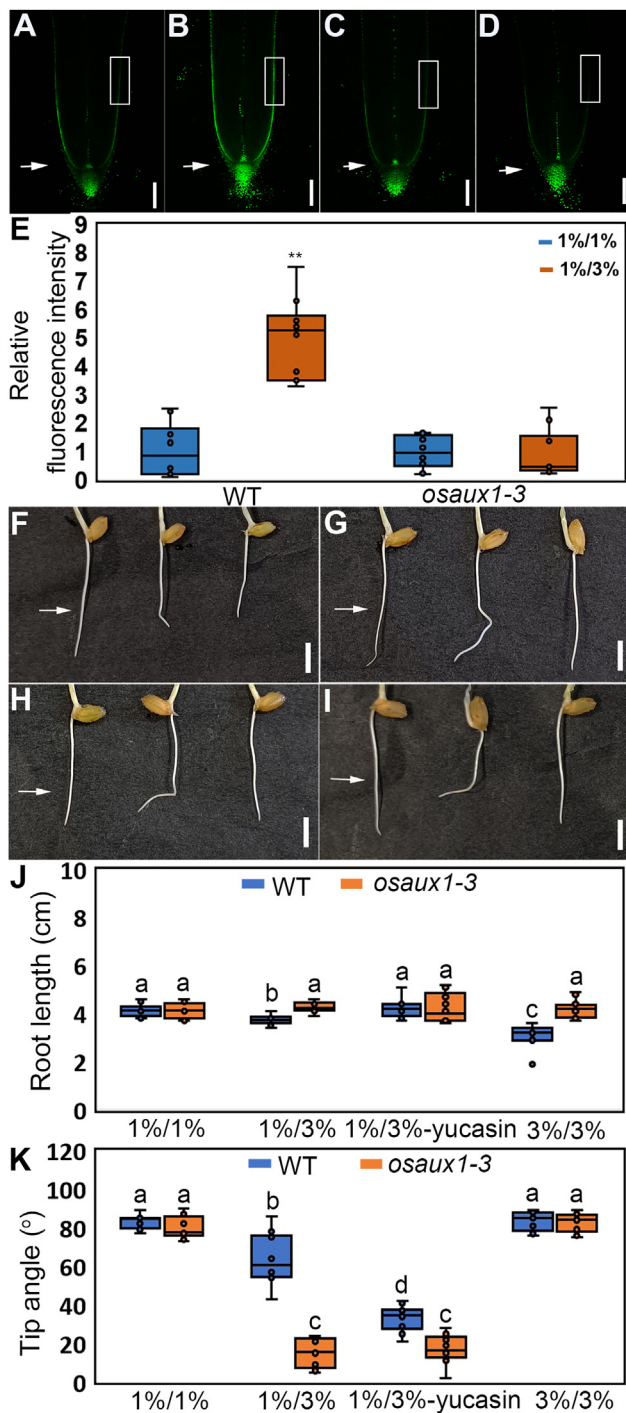


Figure 5. Mutation in *OsAUX1* exhibit defective root penetration into compacted layers

(A–D) Representative confocal images captured at median plane of WT (cv. DJ) and *osaux1-3* primary root tips of rice auxin sensor (DR5-VENUS) cultured in 1%/1% and 1%/3% agar systems. From left to right: WT, 1%/1% (A); WT, 1%/3% (B); *osaux1-3*, 1%/1% (C); *osaux1-3*, 1%/3% (D). Scale bars represent 100 μ m. White arrows indicate the split barrier positions.

(E) Boxplot exhibiting the relative fluorescence intensity of VENUS signals in the root cap of WT and *osaux1-3* grown in 1%/1% and 1%/3% systems. $n = 10$. Student's *t* test: ** $p < 0.01$.

The primary advantage of root hair facilitating root penetration into high-strength layers lies in their ability to increase the number of roots that can successfully penetrate these layers, rather than solely improving the rate of elongation once within the compacted layer. This trait is particularly valuable in agricultural fields, as enhancing root penetration has a significant impact on enlarging the overall root system size and increasing access to soil resources, especially those situated in deeper layers. Additionally, enhanced root penetration ability is imperative for establishment of plants under conditions prone to topsoil drying. Our results provide new insights into a key root trait for breeders to select to enable crops to be more resilient to soil stresses by exploiting variation in root hair length.

STAR★METHODS

Detailed methods are provided in the online version of this paper and include the following:

- KEY RESOURCES TABLE
- RESOURCE AVAILABILITY
 - Lead contact
 - Materials availability
 - Data and code availability
- EXPERIMENTAL MODEL AND SUBJECT DETAILS
 - Plant materials and growth conditions
- METHOD DETAILS
 - Root penetration treatment
 - Soil materials preparation and CT scanning
 - Chemical treatment
 - RNA extraction, RT-PCR, qRT-PCR and vector construct
 - GUS staining
 - Root hair assays
 - Laser scanning microscope assays
 - Accession numbers
- QUANTIFICATION AND STATISTICAL ANALYSIS

SUPPLEMENTAL INFORMATION

Supplemental information can be found online at <https://doi.org/10.1016/j.cub.2024.03.064>.

ACKNOWLEDGMENTS

Prof. Dabing Zhang passed away on June 22, 2023. We dedicate this work to his memory. We thank Prof. Chuanzao Mao for providing *rhl1-1* seeds and Prof. Zhaojun Ding for providing auxin biosynthesis inhibitor, yucasin. This work

(F and G) Representative images of WT primary root grown in uniform (from left to right: 1%/1%, 1%/3%, and 3%/3%) agar systems without (F) or with (G) 20 μ M yucasin. Scale bars represent 1 cm. White arrows indicate the split barrier positions.

(H and I) Representative images of *osaux1-3* primary root grown in uniform (from left to right: 1%/1%, 1%/3%, and 3%/3%) agar systems without (H) or with (I) 20 μ M yucasin. Scale bars represent 1 cm. White arrows indicate the split barrier positions.

(J) Boxplot showing the root growth length of WT and *osaux1-3* grown in 1%/1% and 1%/3% systems with/without 20 μ M yucasin. $n = 12$. Different letters indicate significant differences. $p < 0.01$ from one-way analysis of variance (ANOVA) with Tukey's multiple comparison test.

(K) Boxplot showing the root tip angle of WT and *osaux1-3* grown in 1%/1% and 1%/3% systems with/without 20 μ M yucasin. $n = 12$. Different letters indicate significant differences. $p < 0.01$ from one-way analysis of variance (ANOVA) with Tukey's multiple comparison test.

See also Figures S1 and S2.

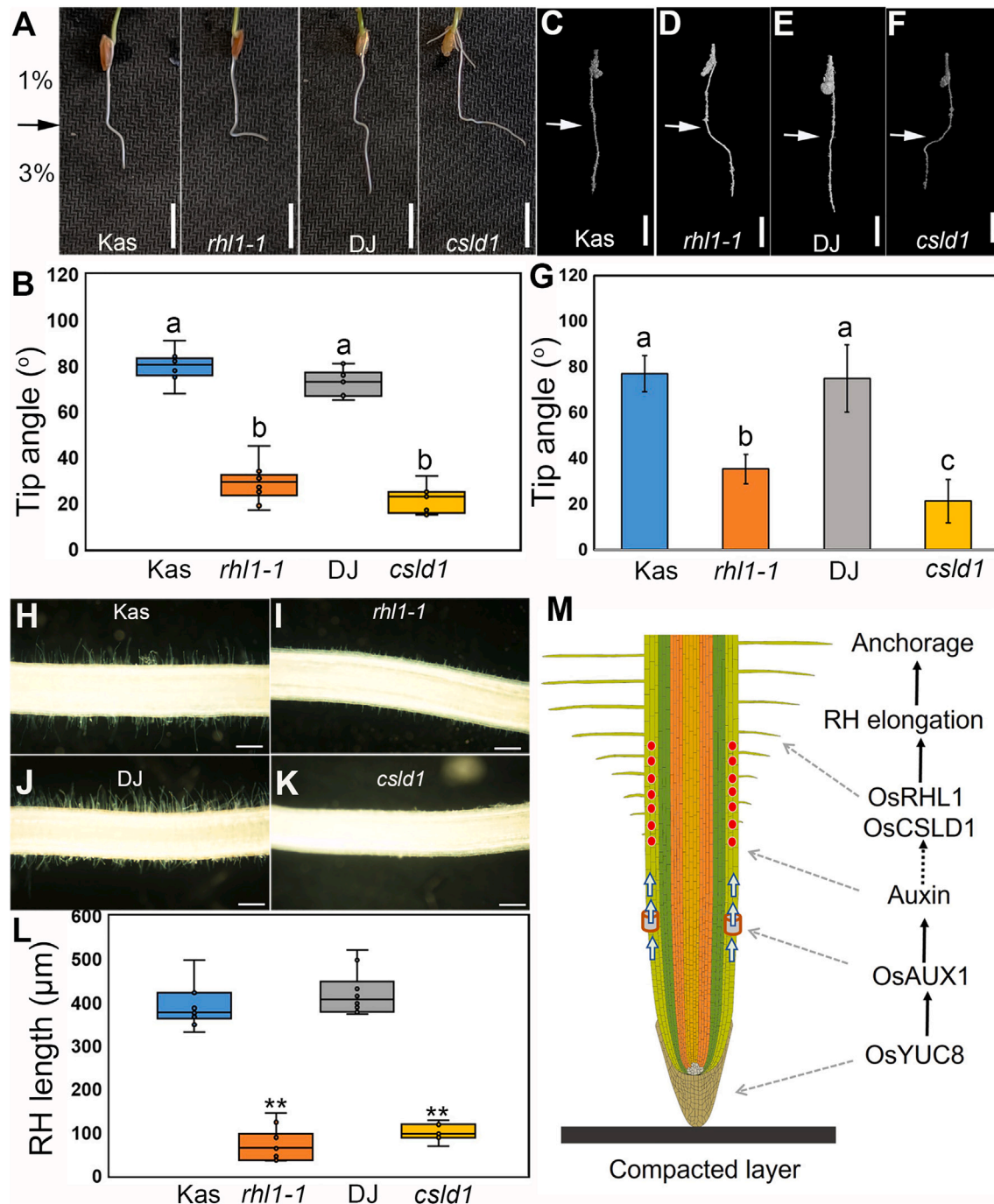


Figure 6. Root hair mutants exhibit impaired root penetration through a compacted layer

(A) Representative images of WT (cv. Kas and DJ) and root hair (RH) mutants (*rh1-1* and *csld1*) primary root tips grown in split (1%/3% agar) system. Scale bars represent 1 cm. Black arrows indicate the split barrier positions.

(B) Boxplot showing the root growth angle of WT and RH mutants (*rh1-1* and *csld1*) grown in split (1%/3%) system. $n = 10$. Different letters indicate significant differences. $p < 0.01$ from one-way analysis of variance (ANOVA) with Tukey's multiple comparison test.

(C and D) Representative images of WT (C) and *rh1-1* (D) seedlings grown in split soils (upper: 1.1_BD; lower: 1.4_BD). Scale bars represent 1 cm. White arrows indicate split barrier positions (see also Videos S1, S2, and S3).

(E and F) Representative images of WT (E) and *csld1* (F) seedlings grown in split soils (upper: 1.1_BD; lower: 1.4_BD). Scale bars represent 1 cm. White arrows indicate split barrier positions (see also Videos S1, S4, and S5).

(G) Angle analysis of WT and RH mutants. Error bars are \pm SD, $n = 3$. Different letters indicate significant differences. $p < 0.01$ from one-way analysis of variance (ANOVA) with Tukey's multiple comparison test.

(H and I) Representative images of WT (H) and *rh1-1* (I) RH at mature stage were captured in split system. Scale bars represent 500 μ m.

(legend continued on next page)

was supported by the National Natural Science Foundation of China (32101651 and 32130006), the Shanghai Rising Star Program (22QA1404200), the China Innovative Research Team, the Ministry of Education, and the Programme of Introducing Talents of Discipline to Universities (111 Project, B14016). B.K.P. acknowledges the support from the BBSRC Discovery Fellowship (BB/V00557X/1) and the Royal Society Research Grant (RGS\R1\231374).

AUTHOR CONTRIBUTIONS

G.H., X.K., B.K.P., and M.J.B. conceptualized the work; X.K., S.Y., Y.X., X.S., L.N.-M., X.W., J.R., and G.H. performed experiments; X.K., S.Y., B.K.P., H.Z., and G.H. performed data analysis; G.H., M.J.B., and H.Z. designed the experiments; G.H., B.K.P., H.Z., and M.J.B. wrote, reviewed, and edited the paper.

DECLARATION OF INTERESTS

The authors declare no competing interests.

Received: October 18, 2023

Revised: March 5, 2024

Accepted: March 28, 2024

Published: April 22, 2024

REFERENCES

- Samson, B.K., Hasan, M., and Wade, L.J. (2002). Penetration of hardpans by rice lines in the rainfed lowlands. *Field Crops Res.* **76**, 175–188.
- Sundaramurthy, V., Ravikummar, V., and Krishnamoorthy, K.K. (1974). Effect of soil compaction on plant growth and yield of cereals. *Madras Agricul. J.* **61**, 893–894.
- Bengough, A.G., and Mullins, C.E. (1990). Mechanical impedance to root growth: a review of experimental techniques and root growth responses. *J. Soil Sci.* **41**, 341–358.
- Young, I.M., Montagu, K., Conroy, J., and Bengough, A.G. (1997). Mechanical impedance of root growth directly reduces leaf elongation rates of cereals. *New Phytol.* **135**, 613–619.
- Tsegaye, T., and Mullins, C.E. (1994). Effect of mechanical impedance on root growth and morphology of two varieties of pea (*Pisum sativum* L.). *New Phytol.* **126**, 707–713.
- Whalley, W.R., Watts, C.W., Gregory, A.S., Mooney, S.J., Clark, L.J., and Whitmore, A.P. (2008). The effect of soil strength on the yield of wheat. *Plant Soil* **306**, 237–247.
- Whalley, W.R., Clark, L.J., Gowing, D.J.G., Cope, R.E., Lodge, R.J., and Leeds-Harrison, P.B. (2006). Does soil strength play a role in wheat yield losses caused by soil drying? *Plant Soil* **280**, 279–290.
- Springmann, M., Clark, M., Mason-D’Croz, D., Wiebe, K., Bodirsky, B.L., Lassaletta, L., de Vries, W., Vermeulen, S.J., Herrero, M., Carlson, K.M., et al. (2018). Options for keeping the food system within environmental limits. *Nature* **562**, 519–525.
- Bello-Bello, E., López-Arredondo, D., Rico-Chambrón, T.Y., and Herrera-Estrella, L. (2022). Conquering compacted soils: uncovering the molecular components of root soil penetration. *Trends Plant Sci.* **27**, 814–827.
- Clark, L.J., Ferraris, S., Price, A.H., and Whalley, W.R. (2008). A gradual rather than abrupt increase in soil strength gives better root penetration of strong layers. *Plant Soil* **307**, 235–242.
- Clark, L.J., Price, A.H., Steele, K.A., and Whalley, W.R. (2008). Evidence from near-isogenic lines that root penetration increases with root diameter and bending stiffness in rice. *Funct. Plant Biol.* **35**, 1163–1171.
- Bengough, A.G., McKenzie, B.M., Hallett, P.D., and Valentine, T.A. (2011). Root elongation, water stress, and mechanical impedance: a review of limiting stresses and beneficial root tip traits. *J. Exp. Bot.* **62**, 59–68.
- Bengough, A.G., Loades, K., and McKenzie, B.M. (2016). Root hairs aid soil penetration by anchoring the root surface to pore walls. *J. Exp. Bot.* **67**, 1071–1078.
- Grierson, C., Nielsen, E., Ketelaarc, T., and Schiefelbein, J. (2014). Root hairs. *Arabidopsis Book* **12**, e0172.
- Pandey, B.K., Huang, G.Q., Bhosale, R., Hartman, S., Sturrock, C.J., Jose, L., Martin, O.C., Karady, M., Voesenek, L.A.C.J., Ljung, K., et al. (2021). Plant roots sense soil compaction through restricted ethylene diffusion. *Science* **371**, 276–280.
- Batey, T., and McKenzie, D.C. (2006). Soil compaction: identification directly in the field. *Soil Use Manag.* **22**, 123–131.
- Whalley, W.R., To, J., Kay, B.D., and Whitmore, A.P. (2007). Prediction of the penetrometer resistance of soils with models with few parameters. *Geoderma* **137**, 370–377.
- Taylor, H.M., and Ratliff, L.F. (1969). Root elongation rates of cotton and peanuts as a function of soil strength and soil water content. *Soil Sci.* **108**, 113–119.
- Jacobsen, A.G.R., Jervis, G., Xu, J., Topping, J.F., and Lindsey, K. (2021). Root growth responses to mechanical impedance are regulated by a network of ROS, ethylene and auxin signalling in Arabidopsis. *New Phytol.* **231**, 225–242.
- Mousavi, S.A.R., Dubin, A.E., Zeng, W.Z., Coombs, A.M., Do, K., Ghadir, D.A., Keenan, W.T., Ge, C.N., Zhao, Y.D., and Patapoutian, A. (2021). PIEZO ion channel is required for root mechanotransduction in Arabidopsis thaliana. *Proc. Natl. Acad. Sci. USA* **118**, e2102188118.
- Tracy, S.R., Black, C.R., Roberts, J.A., McNeill, A., Davidson, R., Tester, M., Samec, M., Korošak, D., Sturrock, C., and Mooney, S.J. (2012). Quantifying the effect of soil compaction on three varieties of wheat (*Triticum aestivum* L.) using X-ray Micro Computed Tomography (CT). *Plant Soil* **353**, 195–208.
- Tracy, S.R., Black, C.R., Roberts, J.A., Sturrock, C., Mairhofer, S., Craigon, J., and Mooney, S.J. (2012). Quantifying the impact of soil compaction on root system architecture in tomato (*Solanum Lycopersicum*) by X-ray micro-computed tomography. *Ann. Bot.* **110**, 511–519.
- Huang, G., Kilic, A., Karady, M., Zhang, J., Mehra, P., Song, X., Sturrock, C.J., Zhu, W., Qin, H., Hartman, S., et al. (2022). Ethylene inhibits rice root elongation in compacted soil via ABA- and auxin-mediated mechanisms. *Proc. Natl. Acad. Sci. USA* **119**, e2201072119.
- Huang, G., Liang, W., Sturrock, C.J., Pandey, B.K., Giri, J., Mairhofer, S., Wang, D., Muller, L., Tan, H., York, L.M., et al. (2018). Rice actin binding protein RMD controls crown root angle in response to external phosphate. *Nat. Commun.* **9**, 2346.
- Mashiguchi, K., Tanaka, K., Sakai, T., Sugawara, S., Kawaide, H., Natsume, M., Hanada, A., Yaeno, T., Shirasu, K., Yao, H., et al. (2011). The main auxin biosynthesis pathway in Arabidopsis. *Proc. Natl. Acad. Sci. USA* **108**, 18512–18517.
- Qin, H., Zhang, Z., Wang, J., Chen, X., Wei, P., and Huang, R. (2017). The activation of OsEIL1 on YUC8 transcription and auxin biosynthesis is required for ethylene-inhibited root elongation in rice early seedling development. *PLoS Genet.* **13**, e1006955.
- Nishimura, T., Hayashi, K., Suzuki, H., Gyojda, A., Takaoka, C., Sakaguchi, Y., Matsumoto, S., Kasahara, H., Sakai, T., Kato, J., et al. (2014). Yucasin is a potent inhibitor of YUCCA, a key enzyme in auxin biosynthesis. *Plant J.* **77**, 352–366.

(J and K) Representative images of WT (J) and *cs1d1* (K) RH at mature stage were captured in split system. Scale bars represent 500 μ m.

(L) RH length analysis of WT and RH mutants in split agar system. $n = 10$. Student’s t test: ** $p < 0.01$.

(M) Schematic representation of root responses in uniform versus split system. Increasing hardness orchestrates the induction of *OsYUC8* expression, which directly upregulates auxin levels of root cap, and then *OsAUX1* facilitates auxin transport from root cap to RH zone, and more auxin promotes RH elongation. Finally, longer RH could anchor growing root tips and provide the force for root penetration.

Related to [Figures S3–S6](#).

28. Giri, J., Bhosale, R., Huang, G., Pandey, B.K., Parker, H., Zappala, S., Yang, J., Dievart, A., Bureau, C., Ljung, K., et al. (2018). Rice auxin influx carrier OsAUX1 facilitates root hair elongation in response to low external phosphate. *Nat. Commun.* **9**, 1408.
29. Ding, W., Yu, Z., Tong, Y., Huang, W., Chen, H., and Wu, P. (2009). A transcription factor with a bHLH domain regulates root hair development in rice. *Cell Res.* **19**, 1309–1311.
30. Kim, C.M., Park, S.H., Je, B.I., Park, S.H., Park, S.J., Piao, H.L., Eun, M.Y., Dolan, L., and Han, C.D. (2007). OsCSLD1, a cellulose synthase-like D1 gene, is required for root hair morphogenesis in rice. *Plant Physiol.* **143**, 1220–1230.
31. Keen, A., Hall, N., Soni, P., Gholkar, M.D., Cooper, S., and Ferdous, J. (2013). A review of the tractive performance of wheeled tractors and soil management in lowland intensive rice production. *J. Terramech.* **50**, 45–62.
32. Vial, L.K., Lefroy, R.D.B., and Fukai, S. (2013). Effects of hardpan disruption on irrigated dry-season maize and on subsequent wet-season lowland rice in Lao PDR. *Field Crops Res.* **152**, 65–73.
33. Barzegar, A.R., Nadian, H., Heidari, F., Herbert, S.J., and Hashemi, A.M. (2006). Interaction of soil compaction, phosphorus and zinc on clover growth and accumulation of phosphorus. *Soil Till. Res.* **87**, 155–162.
34. Kurusu, T., Kuchitsu, K., Nakano, M., Nakayama, Y., and Iida, H. (2013). Plant mechanosensing and Ca²⁺ transport. *Trends Plant Sci.* **18**, 227–233.

STAR★METHODS

KEY RESOURCES TABLE

| REAGENT or RESOURCE | SOURCE | IDENTIFIER |
|--|----------------------------|--------------|
| Bacterial strains | | |
| <i>E. coli</i> (TOP10) | Widely used | N/A |
| <i>Agrobacterium tumefaciens</i> (strain EHA105) | Widely used | N/A |
| Critical commercial assays | | |
| RNeasy Plant Mini | QIAGEN | Cat# 74904 |
| HiScript II Q RT SuperMix for qPCR (+gDNA wiper) | Vazyme | Cat# R223-01 |
| KOD One™ PCR Master Mix | TOYOBO | Cat# KMM-101 |
| Agar (Phytigel) | Sigma | Cat# P8169 |
| ClonExpress II One Step Cloning Kit | Vazyme | Cat# C112-02 |
| Experimental models: Organisms/strains | | |
| Rice: Nipponbare (wild type) | Widely used | N/A |
| Rice: DongJin (wild type) | Widely used | N/A |
| Rice: Hwayoung (wild type) | Widely used | N/A |
| Rice: Kasalath (wild type) | Widely used | N/A |
| Rice: <i>osyuc8-2</i> /HWY | Qin et al. ²⁶ | N/A |
| Rice: <i>osaux1-3</i> /DJ | Giri et al. ²⁸ | N/A |
| Rice: DR5-VENUS | Huang et al. ²⁴ | N/A |
| Rice: <i>oscsld1</i> /DJ | Kim et al. ³⁰ | N/A |
| Rice: <i>osrh1-1</i> /Kas | Ding et al. ²⁹ | N/A |
| Rice: <i>ProRHL1::VENUS-N7</i> | This study | N/A |
| Rice: <i>ProCSLD1::VENUS-N7</i> | This study | N/A |
| Rice: DR5-VENUS/ <i>osyuc8-2</i> | This study | N/A |
| Rice: DR5-VENUS/ <i>osaux1-3</i> | Giri et al. ²⁸ | N/A |
| Rice: <i>ProOsYUC8::GUS</i> | This study | N/A |
| Oligonucleotides | | |
| <i>OsYUC3</i> qRT-PCR Forward: GTGAGAACGGGCTCTACTCGGTCG | This paper | N/A |
| <i>OsYUC3</i> qRT-PCR Reverse: GCTTATGCATGACCGATGAACACG | This paper | N/A |
| <i>OsYUC5</i> qRT-PCR Forward: GAGAAATACGGCCTCCGACG | This paper | N/A |
| <i>OsYUC5</i> qRT-PCR Reverse: CGACCCATCCTCTGTGAAG | This paper | N/A |
| <i>OsYUC8</i> qRT-PCR Forward: CCAACATCTCCTCGGTGTAG | This paper | N/A |
| <i>OsYUC8</i> qRT-PCR Reverse: GCATCAGACAAGCAACATCC | This paper | N/A |
| <i>OsYUC11</i> qRT-PCR Forward: ATGCCCAAGAAGGACTTCCC | This paper | N/A |
| <i>OsYUC11</i> qRT-PCR Reverse: GAAGGCCTTGACGTCATTAGCA | This paper | N/A |
| <i>OsIAA20</i> qRT-PCR Forward: CGGGATTATTTGTTCCACGTTTC | This paper | N/A |
| <i>OsIAA20</i> qRT-PCR Reverse: CGAGATTTTCATTGTCATGCTTA | This paper | N/A |
| <i>TUB</i> qRT-PCR Forward: GCTGACCACACCTAGCTTTGG | This paper | N/A |

(Continued on next page)

Continued

| REAGENT or RESOURCE | SOURCE | IDENTIFIER |
|---|-------------|---|
| TUB qRT-PCR Reverse: AGGGAACCTTAGGCAGCATGT | This paper | N/A |
| Software | | |
| ImageJ | Widely used | https://imagej.nih.gov/ij/ |
| Excel 2023 | Widely used | N/A |

RESOURCE AVAILABILITY**Lead contact**

Further information and requests for resources and reagents should be directed to and will be fulfilled by the lead contact, Guoqiang Huang (huang19880901@sjtu.edu.cn).

Materials availability

DNA constructs and transgenic rice seeds generated in this study are available from the [lead contact](#), Guoqiang Huang, upon request.

Data and code availability

- All data reported in this paper will be shared by the [lead contact](#) upon request.
- This paper does not report original code.
- Any additional information required to reanalyze the data reported in this paper is available from the [lead contact](#) upon request.

EXPERIMENTAL MODEL AND SUBJECT DETAILS**Plant materials and growth conditions**

The genetic backgrounds of rice cultivars are Dong Jin (DJ) (*Oryza sativa*, *Japonica*), Kasalath (Kas) (*Oryza sativa*, *Indica*) and Hwayoung (HWY) (*Oryza sativa*, *Japonica*). *Osaux1-3* and *csld1* are two T-DNA insertion mutants under DJ background. *Osyuc8-2* is a T-DNA insertion mutant in HWY background. *rhl1-1* harbors a point mutation disrupting the splicing site and causing a shift in the reading frame. All rice plants were cultured in Shanghai (31°3' N, 121°44' E) and Sanya (8°33' N, 109°16' E), China, in the summer and winter seasons, respectively. The seedlings were cultured in a light incubator with 18h-lightness/6h-darkness at 28 °C.

METHOD DETAILS**Root penetration treatment**

The rice seeds were dipped into the water under dark for 4 days at 28 °C. The germinated seeds were transferred and inserted into the medium containing 1% (w/v)/1%, 1%/3% and 3%/3% low-melting agars (pH = 5.8) melted by ddH₂O. The germinated seeds were cultured at 12-h lightness/12-h darkness at 28 °C. After 5-day growth, the excess agar around the root system was carefully chopped with maintaining its original growth state, then the closely surrounding agar was melted and then removed by 50 °C heat treatment for 5 min prior to imaging. Finally, the seedlings were used to be imaged and analyzed. The root length and growth angle were calculated via ImageJ (<https://imagej.nih.gov/ij/>).

Soil materials preparation and CT scanning

Soil was collected from Yingtian, Jiangxi Province, CHN (28°15' N, 116°5' E), passed through a 2 mm sieve. Soil basic properties: pH 4.9, soil organic carbon 10.23 g kg⁻¹, total nitrogen 0.90 g kg⁻¹, available phosphorus 34.15 mg kg⁻¹, available potassium 235.11 mg kg⁻¹. Equally germinated seedlings of WT and mutants were grown in columns (60 mm diameter x 130 mm height) filled with the soil packed to a bulk density of either 1.0 g cm⁻³ (noncompacted) or 1.4 g cm⁻³ (compacted). These plants were grown in a controlled growth chamber maintained at 28 °C, 16-hour photoperiod with 70% relative humidity. The root systems of 5-day-old seedlings were imaged non-destructively using an Xradia 520 Versa (Carl Zeiss, Germany) based at INSTRUMENTAL ANALYSIS CENTER, Shanghai Jiao Tong University. Scans were acquired by collecting 1200 projection images at 140 kV X-ray energy. Scan resolution was 40 microns. Image reconstruction was performed using Datos|REC software (GE Inspection Technologies, Wunstorf, Germany) and roots were visualized and measured using the polyline tool in VGStudioMax (Volume Graphics GmbH, Germany).

Chemical treatment

Rice seeds (WT, *osyuc8-2*, and *osaux1-3*, and other mutants) were germinated for 4 days in water at 28 °C. The germinated seeds were transferred and inserted into the medium with/without 20 μM yucasin (5-(4-chlorophenyl)-4H-1,2,4-triazole-3-thiol (WAKO, 352-12001)) or 10 nM NAA. After 5-day growth, the roots were imaged and analyzed as above description.

RNA extraction, RT-PCR, qRT-PCR and vector construct

The samples were harvested from 0 to 5 mm distal from the primary root tips of the 5-day-old seedlings when root encountering the mechanical impedance. Total RNA was extracted using TRIzol reagent (Invitrogen) with accordance to the instruction of manufacturer. 1 μg RNA was used to synthesize the first strand cDNA using the Rever Tra Ace-a-First strand cDNA synthesis kit (Vazyme). The quantitative RT-PCR (qRT-PCR) analysis was conducted as previously described.²⁴ The rice *TUB* gene was used as internal control.

All PCR amplifications were done with KOD ONE DNA polymerases (TOYOBO) with the recommended annealing temperature and extension time. Sequences were analyzed with SnapGene. PCR products were recovered with QIAquick® Spin miniprep kit, and DNA midpreps were with the Qiagen TIP-100 kit. The function *proYUC8::GUS* reporter construct was constructed via the ClonExpress II One Step Cloning Kit (Vazyme). For this vector, more than 15 independent transgenic lines were obtained for each vector. One representative transgenic plant was used for further analysis.

GUS staining

The roots of 5-day-old *ProOsYUC8::GUS* transgenic plants were immersed into GUS solution (50 mM Na₃PO₄ (pH 7.0), 50 mM NaH₂PO₄, 10 mg/mL X-Gluc and 0.02% (v/v) TritonX-100, 10 mM Na₂EDTA, 0.5 mM K₃[Fe(CN)₆], 0.5 mM K₄[Fe(CN)₆]) under dark at 37 °C for 12 h. After that, the samples were washed with 70% ethanol for 36 h. The GUS staining images were taken via Leica light microscope (M205A) with a CCD camera.

Root hair assays

The rice seeds were germinated in the water under dark for 4 days at 28 °C. Uniformly germinating seeds were inserted into the agar system. After 5-day growth, the excess agar around the root system was carefully punctured without disrupting its original growth state, then the closely surrounding agar was melted and removed by 50 °C heat treatment for further imaging. Root hair was recorded on elongated zone of the primary root using a Leica transmission microscope (dark field). Root hair length was measured as the average of 10 fully elongated root hairs of one seedling via ImageJ (<https://imagej.nih.gov/ij/>).

Laser scanning microscope assays

Auxin response DR5-VENUS reporter seeds were germinated in dark for 4 days and then transferred into different densities of agar to grow for another 5 days under 28 °C. The roots were extracted from the agars and used to be observed via Leica Laser Scan Microscope (SP5) using an excitation wavelength of 488 nm and emission wavelength of 500-550 nm. Confocal images were analyzed via ImageJ (<https://imagej.nih.gov/ij/>).

Accession numbers

OsYUC3 (Os01g0732700); *OsYUC5* (Os12g0512000); *OsYUC8* (Os03g0162000); *OsYUC11* (Os12g0189500); *OsRHL1* (Os06g0184000); *OsCSLD1* (Os10g0578200); *OsAUX1* (Os01g0856500).

QUANTIFICATION AND STATISTICAL ANALYSIS

Statistical analyses were performed using *Excel* (2023). Data collection and analyses were performed by investigators blinded to the experimental conditions. Experiments were randomized whenever possible. All experiments were replicated in multiple subject rice plants with similar results. All of the statistical details, including the statistical tests used, exact value of n, etc., can be found in main (or supplementary) figure legends. $P < 0.05$ was regarded as statistically significant.

Current Biology, Volume 34

Supplemental Information

**Root hairs facilitate rice root penetration
into compacted layers**

Xiuzhen Kong, Suhang Yu, Yali Xiong, Xiaoyun Song, Lucia Nevescanin-Moreno, Xiaoqing Wei, Jinliang Rao, Hu Zhou, Malcolm J. Bennett, Bipin K. Pandey, and Guoqiang Huang

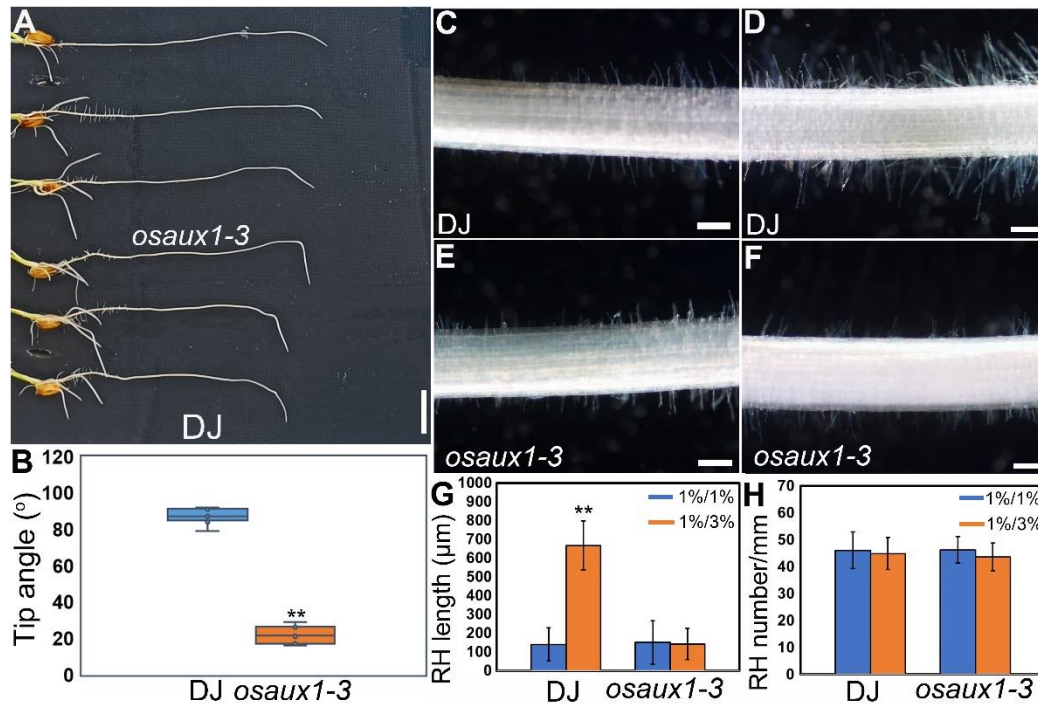


Figure S1 *OsAUX1* mutant exhibits reduced gravitropic responses and RH length. Related to Figure 1.

(A) Representative images of WT (cv DJ) and *osaux1-3* primary roots exposed to 8-hour gravity stimulation. Scale bar, 1 cm.

(B) Tip angle analysis of WT and *osaux1-3* after 8-hour gravitropism. n = 10. Student's *t*-test: ** $P < 0.01$.

(C-D) Representative images of WT root hair (RH) grown in 1%/1% (C) and 1%/3% (D) systems. Scale bars, 500 μm.

(E-F) Representative images of *osaux1-3* RH grown in 1%/1% (E) and 1%/3% (F) systems. Scale bars, 500 μm.

(G-H) Quantitative analysis of RH length (G) and number (H) of WT and *osaux1-3* grown in 1%/1% and 1%/3% systems. Error bars are \pm SD, n = 10. Student's *t*-test: ** $P < 0.01$.

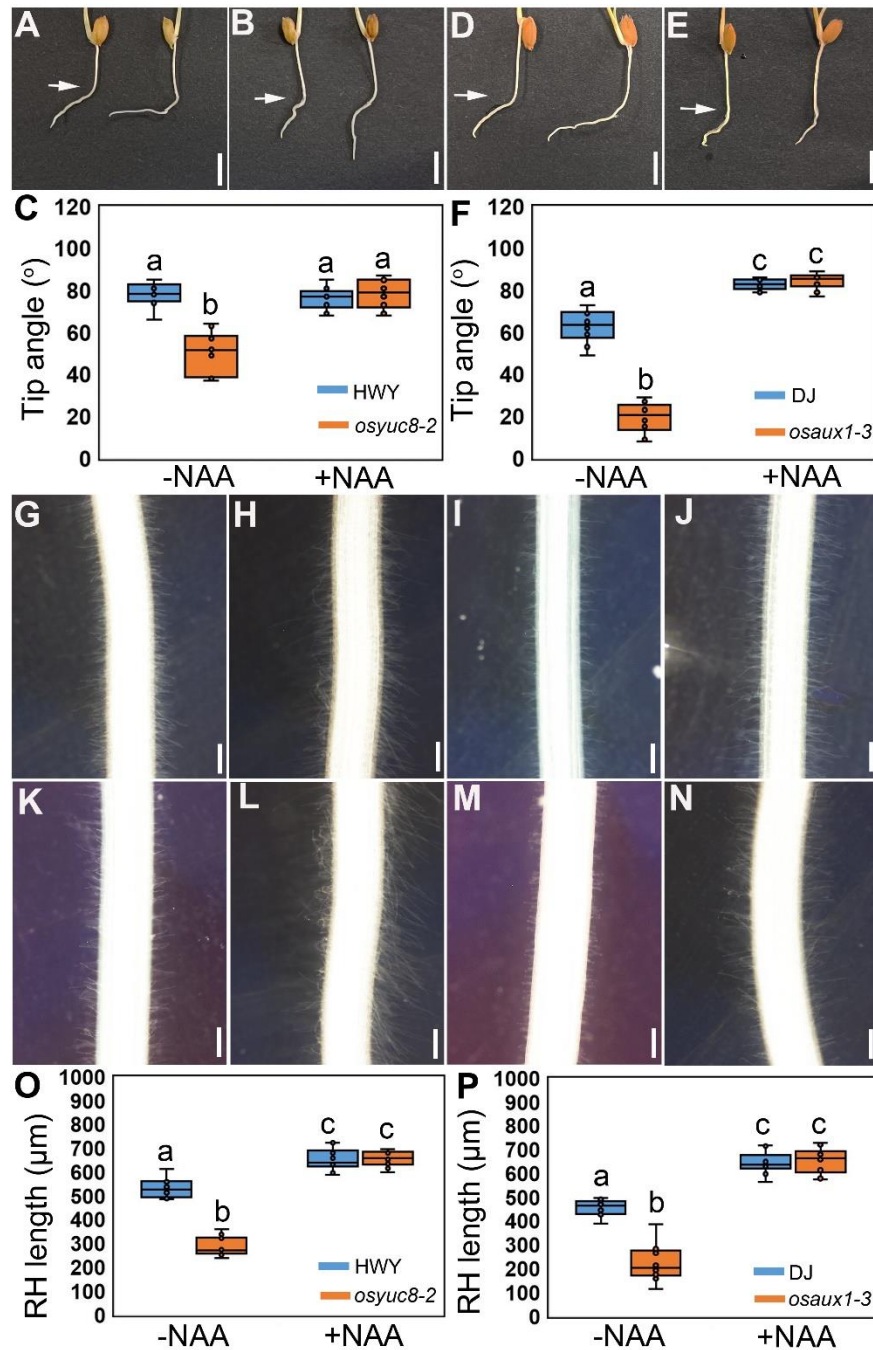


Figure S2 Auxin treatment restores the defects of *osyuc8-2* and *osaux1-3*. Related to Figures 1 and 3.

(A-B) Representative images of WT (cv HWY, left) and *osyuc8-2* (right) primary roots grown in 1%/3% systems without (A) or with (B) 10 nM NAA treatment. Scale bar, 1 cm. White arrows indicate split barrier positions.

(C) Tip angle analysis of WT and *osyuc8-2* grown in 1%/3% systems with and without 10 nM NAA treatment. Different letters indicate significant differences, $P < 0.01$ from one-way analysis of variance (ANOVA) with Tukey's multiple comparison test. $n = 10$.

(D-E) Representative images of WT (cv DJ, left) and *osaux1-3* (right) primary roots grown in 1%/3% systems without (D) or with (E) 10 nM NAA treatment. Scale bar, 1 cm. White arrows indicate split barrier positions.

(F) Tip angle analysis of WT and *osaux1-3* grown in 1%/3% systems with or without 10 nM NAA treatment. Different letters indicate significant differences, $P < 0.01$ from one-way analysis of variance (ANOVA) with Tukey's multiple comparison test. $n = 10$.

(G-H) Representative images of WT root hair (RH) at 1%/3% systems without (G) or with (H) 10 nM NAA treatment. Scale bars represent 500 μm .

(I-J) Representative images of *osyuc8-2* RH at 1%/3% systems without (I) or with (J) 10 nM NAA treatment. Scale bars represent 500 μm .

(K-L) Representative images of WT RH at 1%/3% systems without (K) or with (L) 10 nM NAA treatment. Scale bars represent 500 μm .

(M-N) Representative images of *osaux1-3* RH at 1%/3% systems without (M) or with (N) 10 nM NAA treatment. Scale bars represent 500 μm .

(O-P) Box plot showing RH length analysis of WT, *osyuc8-2* (O), and *osaux1-3* (P) grown in split agar systems with and without 10 nM NAA treatment. $n = 10$ representative RHs from 10 individual roots. Different letters indicate significant differences, $P < 0.01$ from one-way analysis of variance (ANOVA) with Tukey's multiple comparison test.

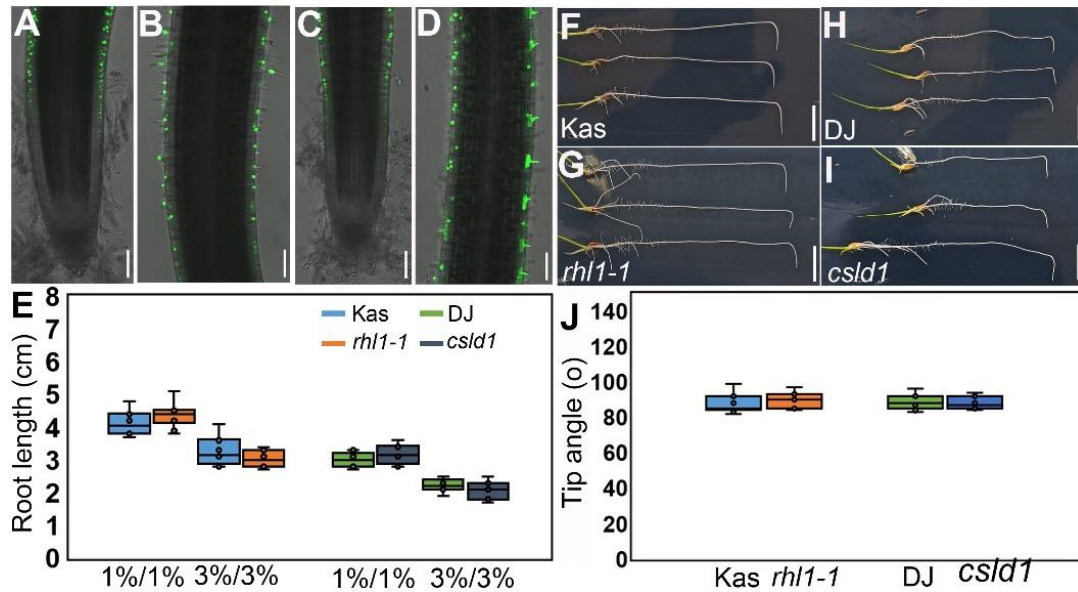


Figure S3 Root hair mutants exhibit normal root elongation and gravitropic responses. Related to Figure 6.

(A-B) Representative images of rice *proRHL1::VENUS-N7* transcriptional reporter. Scale bars, 100 μ m.

(C-D) Representative images of rice *proCSLD1::VENUS-N7* transcriptional reporter. Scale bars, 100 μ m.

(E) Box plot showing the primary root length of WT (cv Kas and DJ) and RH mutants (*rhl1-1* and *csld1*) grown in uniform (1%/1% and 3%/3% agar) system. n = 10.

(F-G) Representative images of WT (cv. Kas) (F) and *rhl1-1* (G) seedlings after 8-hour gravitropic stimuli. Scale bars, 1 cm.

(H-I) Representative images of WT (cv. DJ) (H) and *csld1* (I) seedlings after 8-hour gravitropic stimuli. Scale bars, 1 cm.

(J) Gravitropic angle analysis of WT and RH mutants. n = 11.

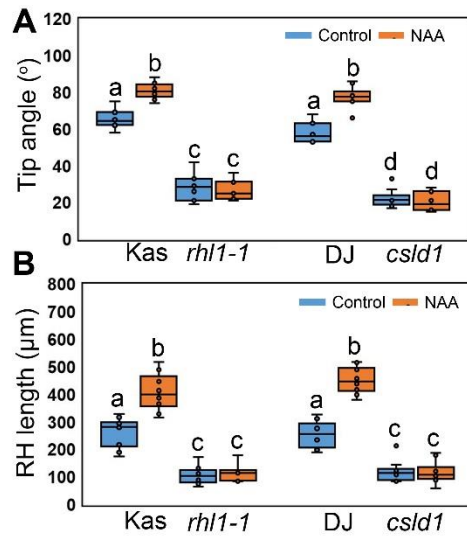


Figure S4 Root hair mutants exhibit less response to auxin treatment. Related to Figure 6.

(A) Tip angle analysis of WT (cv Kas and DJ) and root hair (RH) mutants grown in 1%/3% systems with and without 10 nM NAA treatment. Different letters indicate significant differences, $P < 0.01$ from one-way analysis of variance (ANOVA) with Tukey's multiple comparison test. $n = 10$.

(B) Box plot showing RH length analysis of WT (cv Kas and DJ) and RH mutants grown in 1%/3% systems with and without 10 nM NAA treatment. Different letters indicate significant differences, $P < 0.01$ from one-way analysis of variance (ANOVA) with Tukey's multiple comparison test. $n = 10$.

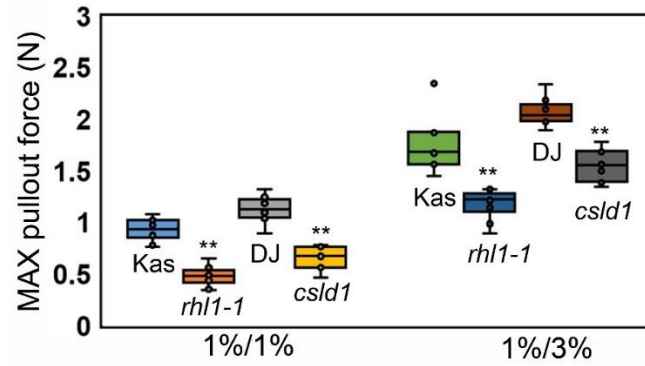


Figure S5 Box plot of peak force required to pull the roots from the system. Related to Figure 6.

Mean force for WT (cv Kas and DJ) is ~1 N in 1%/1%, to a maximum of ~2 N in 1%/3%. The mean maximum pull-out force for hairless mutants was significantly smaller than the WT for the same treatment. n = 10. Student's *t*-test: ** $P < 0.01$.

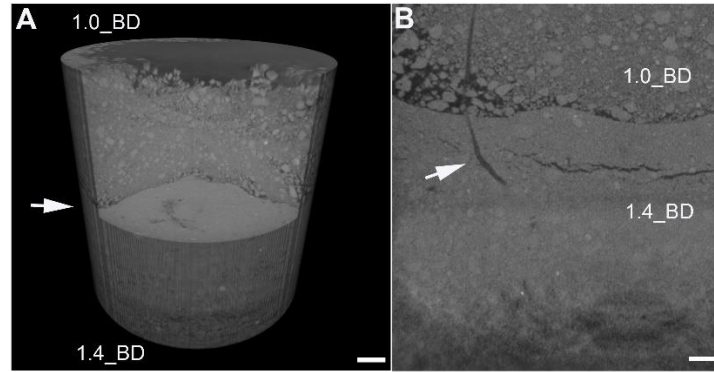


Figure S6 Microstructure of loamy clay soil cores in split system used in this work. Related to Figure 6.

(A) Three-dimensional visualization of the soil column used in this work. Upper soil: 1.0_BD; Lower soil: 1.4_BD. White arrow indicates the boundary between 1.0_BD soil and 1.4_BD soil. Scale bar, 2 cm.

(B) CT images showing soil profile of the split system. White arrow indicates the rice root imaged in this system. Scale bar, 1 cm.